

Original article

Synthesis, antitubercular activity and docking study of novel cyclic azole substituted diphenyl ether derivatives

Suvarna G. Kini ^{a,*}, Anilchandra R. Bhat ^b, Byron Bryant ^c,
John S. Williamson ^c, Franck E. Dayan ^d^a Department of Pharmaceutical Chemistry, Manipal College of Pharmaceutical Sciences, Manipal – 576 104, Karnataka, India^b Department of Pharmaceutical Chemistry, K.L.E.'s College of Pharmaceutical Sciences, Belgaum – 560 010, Karnataka, India^c Department of Medicinal Chemistry, University of Mississippi, University, MS 38677, USA^d USDA-ARS Natural Products Utilization Research Unit, University, MS 38677, USA

Received 17 October 2007; received in revised form 28 March 2008; accepted 8 April 2008

Available online 1 May 2008

Abstract

The re-emergence of tuberculosis (TB) as a global health problem over the past few decades, accompanied by the rise of drug-resistant strains of *Mycobacterium tuberculosis*, emphasizes the need for discovery of new therapeutic drugs against this disease. The emerging serious problem both in terms of TB control and clinical management prompted us to synthesize a novel series of heterocyclic *o*/*m*/*p* substituted diphenyl ether derivatives and determine their activity against H37Rv strain of *Mycobacterium*. All 10 compounds inhibited the growth of the H37Rv strain of mycobacterium at concentrations as low as 1 µg/mL. This level of activity was found comparable to the reference drugs rifampicin and isoniazid at the same concentration. Molecular modeling of the binding of the diphenyl ether derivatives on enoyl-ACP reductase, the molecular target site of triclosan, indicated that these compounds fit within the binding domain occupied by triclosan. Hence the diphenyl ether derivatives tested in this study were docked to ENR and the binding of the diphenyl ether derivatives was also estimated using a variety of scoring functions that have been compiled into the single consensus score. As the scores ranged from 47.27% to 65.81%, these bioactive compounds appear to have a novel mechanism of action against *M. tuberculosis*, and their structural features should be studied further for their potential use as new antitubercular drugs.

© 2008 Elsevier Masson SAS. All rights reserved.

Keywords: Tuberculosis; Enoyl-ACP reductase; Antitubercular activity; Docking

1. Introduction

Tuberculosis (TB) is a chronic infectious disease caused by mycobacteria of the “tuberculosis complex”, including primarily *Mycobacterium tuberculosis*, but also *Mycobacterium bovis* and *Mycobacterium africanum* [1,2]. In the last decade, TB has re-emerged as one of the leading causes of death worldwide (nearly 3 million deaths annually) [3]. The estimated 8.8 million new cases every year correspond to 52,000 deaths per week or more than 7,000 each day [4,5].

These numbers however, are only a partial depiction of the global TB threat. More than 80% of TB patients are in the economically productive age of 15–49 years, which results in tremendous economic and social problems.

It was estimated that nearly 1 billion more people will be infected with TB in the next 20 years. About 15% of that group (150 million) will exhibit symptoms of the disease, and about 3.6% (36 million) will die from TB if new disease prevention and treatment measures are not developed [6]. In 2005, the TB incidence rate was stable or in decline in all six WHO regions, and had reached a peak worldwide. However, the total number of new TB cases is still rising slowly, because the case-load continues to grow in the African, Eastern Mediterranean and South-East Asia regions [6]. The

* Corresponding author. Tel.: +91 820 257 1201x22482; fax: +91 820 2571998.

E-mail address: suvarna_kini@yahoo.com (S.G. Kini).

dramatic increase in TB cases observed in the recent years is a result of two major factors. First is the increased susceptibility of people infected with Acquired Immunodeficiency Syndrome (AIDS) to TB, which augments the risk of developing the disease 100-fold [7]. Second is the increase in resistant strains of the disease [8] with some showing cross-resistance to as many as nine drugs [7].

Although one possible long term solution to the problem is a better vaccine, in the short term, the major reliance will be on chemotherapy [9] requiring the development of novel, effective and non-toxic antitubercular agents [9–11]. The identification of novel target sites will also be needed to circumvent the problems associated with the increasing occurrence of multi-drug resistant strains. To do this, biochemical pathways specific to the mycobacteria and related organisms' disease cycle must be better understood. Many unique metabolic processes occur during the biosynthesis of mycobacterial cell wall components [12]. One of these attractive targets for the rational design of new antitubercular agents are the mycolic acids, the major components of the cell wall of *M. tuberculosis* [13].

Mycolic acids are high molecular weight C74–C90 α -alkyl, β -hydroxy fatty acids covalently linked to arabinogalactan [13–15]. They represent the major lipid components of the mycobacterial cell walls and are unique to mycobacteria and related species [16]. Enzymes that comprise the fatty acid synthetase (FAS) complex responsible for fatty acid biosynthesis are considered ideal targets for designing new antibacterial agents. Enoyl-ACP reductase (ENR) is a key regulatory enzyme in fatty acid elongation, and it catalyses the NADH-dependent stereospecific reduction of α,β -unsaturated fatty acids bound to the acyl carrier protein [17–19]. Two studies have shown that 5-chloro-pyrazinamide (5-Cl-PZA) [20,21] and pyrazinamide (PZA) [21] inhibit *M. tuberculosis* FAS I, indicating that FAS I is also a good drug target.

The diphenyl ether, triclosan 5-chloro-2-(2,4-dichlorophenoxy) phenol ether, is a broad-spectrum biocide that has been used for over 30 years mainly as a component of antimicrobial wash in consumer products such as toothpastes, mouthwashes, deodorant soaps, lotions, children toys and cutting boards [22].

Until recently, it was thought that triclosan, being a relatively small hydrophobic molecule, was absorbed via diffusion into the bacterial cell wall and that its antibacterial activity was the result of a non-specific disruption of the organism's cell wall [23,24]. However, the first evidence that this diphenyl ether inhibits fatty acid biosynthesis came when a genetic analysis of an *Escherichia coli* strain resistant to triclosan linked the resistance to the FabI gene which encodes for ENR [25]. Subsequently extensive biochemical and structural studies have been performed to confirm that triclosan is a specific inhibitor of *E. coli* ENR [18,26–28]. Triclosan also directly inhibits ENR from *Staphylococcus aureus* [29], *Haemophilus influenzae* [30], *M. tuberculosis* and *Mycobacterium smegmatis* (encoded by InhA) [31–33] and *Plasmodium falciparum*, the malarial parasite [34–36]. The common theme in the inhibition of ENRs by triclosan is the requirement of the NAD⁺ cofactor. The interaction of triclosan with ENR is

stabilized by the π – π stacking interaction between the hydroxyl chloro phenyl ring (ring A in Fig. 1) and the hydroxyl group of a tyrosine from hydrogen bonding interactions with the hydroxyl group of triclosan. Ring B of triclosan makes several hydrophobic contacts with ENR. The ether oxygen of triclosan may also be critical in the formation of the stable ENR–triclosan–NAD⁺ complex, since the replacement of the group by a sulfur atom abolishes the inhibitory activity [26].

2. Chemistry

Since diphenyl ethers (including triclosan) are well known for their antitubercular activities [37] and that their mode of action has been characterized, our work has focused on the synthesis of antimycobacterial compounds based on the diphenyl ether skeleton and the synthesized compounds were tested then for their in vitro antitubercular activity. The synthetic pathways are illustrated in Schemes 1 and 2. Molecular modeling of their binding to ENR was also performed to study whether this target was the ideal site to exhibit their mechanism of antitubercular activity.

3. Antitubercular activity and docking studies

3.1. Antitubercular activity

Antitubercular activity of the set of diphenyl ether derivatives was tested using the Lowenstein–Jensen medium (L.J. medium) method [47]. Briefly, eggs were broken aseptically to obtain 200 mL of egg solution. The solution was filtered through a sterile muslin cloth into a sterile conical flask containing glass beads. Sterilized mineral salt solution (120 mL) (consisting of 4.0 g potassium phosphate (anhydrous), 0.4 g of magnesium sulfate, 1.6 g magnesium citrate, 6.0 g of asparagine, 20 mL of glycerol, distilled water to fill to 1 L) and 4 mL of sterilized malachite green solution (2.0%) were added to the 200 mL of egg solution. The contents were mixed well to form a uniform medium.

Compounds (10 mg) were dissolved in 10.0 mL of DMSO and were diluted with DMSO to make 100 μ g/mL and 10 μ g/mL stock solutions. A 0.8 mL aliquot of each concentration was transferred into different McCartney bottles. To this, 7.2 mL of L.J. medium was added and mixed well.

INH and rifampicin (10 mg) were chosen as the standard drugs for the comparison of antitubercular activity. The drug was dissolved in DMSO and diluted and tested as described above. The bottles were incubated at 75–80 °C for 3 days for solidification and sterilization.

Procedure for inoculation. A sweep from H37Rv strain of *M. tuberculosis* culture was discharged with the help of 22

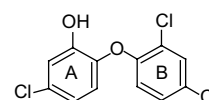
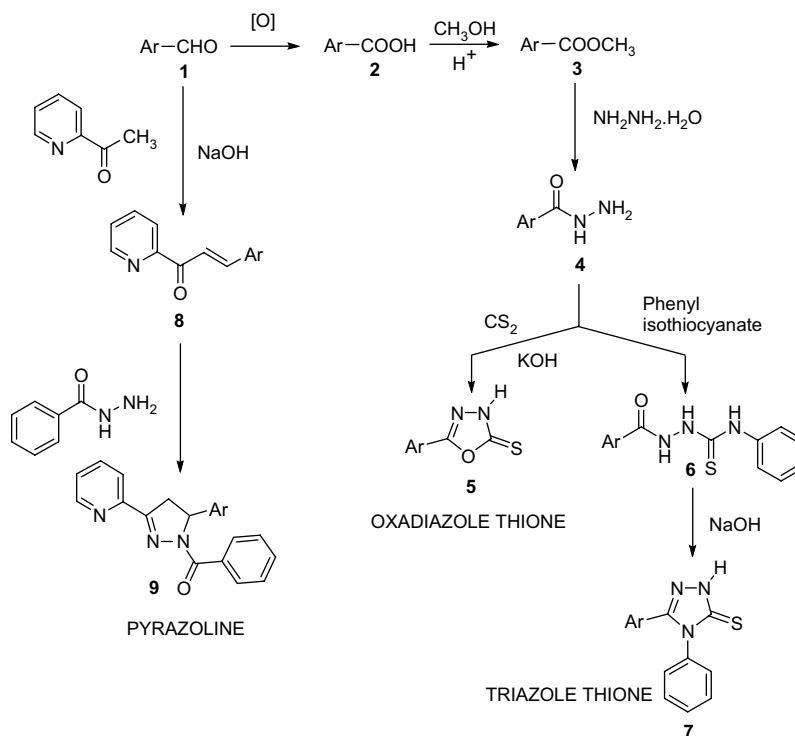


Fig. 1. Structure of triclosan.



Scheme 1. Synthesis of the oxadiazole thiones, triazoles, and pyrazoline derivatives of diphenyl ethers, where Ar = *o*-, *m*-, or *p*-phenoxy phenyl (**a**, **b**, **c**) in case of oxadiazolethione (**5a**, **5b**, and **5c**) and triazole derivatives (**7a**, **7b**, and **7c**) and Ar = *m*-phenoxy phenyl (**9**).

S.W.nichrome wire loop of 3 mm external diameter into a sterile bijou bottle containing six 3 mm glass beads and 4 mL of sterile distilled water. Each loop of culture delivered approximately 4 mg of bacilli cells. The bottle was shaken with the help of a mechanical shaker for 2 min to constitute the suspension. The suspension was inoculated on the surface of each L.J. medium containing the test compounds using 27 S.W.G nichrome wire loop of 3 mm external diameter. L.J. medium containing INH and rifampicin as well as the medium containing DMSO (control) were inoculated with the test organism for positive and negative controls. Medium without any test compound/DMSO was also inoculated with the test organism to check whether the media supports the growth of the tubercle bacilli or not. The inoculated bottles were incubated at 37 °C for 6 weeks, at the end of which readings were taken.

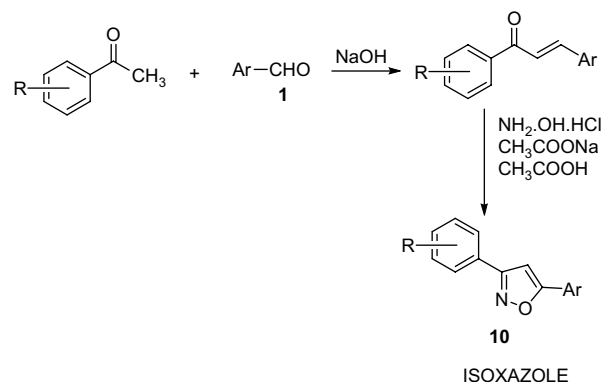
3.2. Computer modeling of ENR and docking of the diphenyl ether data set

The X-ray crystal coordinates of *E. coli* ENR–NAD⁺–triclosan complex at a resolution of 2.0 Å from Qiu et al. [39] were obtained from the Protein Data Bank (<http://www.rcsb.org>) under the accession code 1C14.pdb. Using the program Sybyl 6.9 (Tripos Inc., St. Louis, MO) on a Silicon Graphics O2 250 MHz R10000 workstation, mislabeled atom types from the pdb files were first corrected. Subsequently, proline Φ angles were fixed at 70°, side chain amides were checked to maximize potential H-bonding, side chains were checked for close van der Waals contacts, and essential

hydrogens were added. The model was checked for conformational problems using the module ProTable from Sybyl. Ramachandran plot [48,49] of the backbone torsion angles PHI and PSI, local geometry and the location of buried polar residues/exposed non-polar residues were examined.

The structure was then subjected to an energy refinement procedure. Gasteiger–Huckel charges [49] were calculated for the ligand, while Kollman charges [50] were used for the protein. The model was then subjected to energy minimization following the gradient termination of the Powell method for 3000 iterations using Kollman united force field with non-bonding cutoff set at 9.0 and the dielectric constant set at 4.0.

The 3-D structure of triclosan was obtained from its X-ray crystal coordinate found in 1C14.pdb file. The 3-D structures



Scheme 2. Synthesis of isoxazoles, where Ar = *m*-phenoxy phenyl; R = H (**10a**), 4-chloro (**10b**), and 4-methoxy (**10c**).

of the diphenyl derivatives tested in this study were derived from the coordinate of the triclosan backbone.

3.3. Docking experiment

The diphenyl ether derivatives tested in this study were docked to ENR using FlexX in Sybyl. This software uses an incremental construction approach to place ligands into a binding domain of a protein [51]. The first phase of the FlexX process consists of establishing the base selection where a part of the ligand is selected as a base fragment based on its placeability and specificity [52]. This fragment is then placed into binding domain independently of the rest of the ligand using the pose clustering pattern recognition technique, which optimizes the number of favorable interactions that can occur between the fragment and the protein. Finally, the rest of the ligand is built into the site using the different placements of the base fragment as starting points. The FlexX scoring function uses a modified version of the Böhm function designed for the *de novo* design program LUDI that estimates the free binding energy ΔG of the protein–ligand complex [40].

The binding of the diphenyl ether derivatives was also estimated using a variety of scoring functions that have been compiled into the single consensus score (CScore). The CScore module available in Sybyl includes the G_Score, PMF_Score, D_Score, ChemScore, and the FlexX F_Score scoring functions.

4. Results and discussion

A series of cyclic azole substituted diphenyl ether derivatives were synthesized using *o*-, *m*-, or *p*-phenoxy benzaldehydes with different reagents to form the desired heterocyclic diphenyl ether derivatives. Compounds of type **5** possessed an oxadiazolethione group; compounds of type **7** consisted of a triazole ring, compound **9** with pyrazoline and compounds of type **10** possessed isoxazole ring. Overall, the yields were in the range of 60–88% and the compounds were easy to crystallize. Their structures were confirmed by GC–MS, LC–MS, ^1H NMR and IR spectroscopies (given in synthetic procedure).

The compounds listed in Table 1 were evaluated for antitubercular activity. All 10 diphenyl ether derivatives were highly active against the H37Rv strain *M. tuberculosis* (Table 2). The compounds inhibited the growth of the human pathogen at concentrations as low as 1 $\mu\text{g/mL}$. A concentration of 1 $\mu\text{g/mL}$ corresponds to 3.7 μM for the compounds in **5**, 2.9 μM for compounds in **7**, and 2.4, 3.2, 2.9 and 2.9 μM for compounds **9**, **10a**, **10b**, and **10c**, respectively. Such level of antitubercular activity is comparable to other standard drugs such as isoniazid and rifampicin, which have MICs at 0.01–1.25 and 0.06–0.25 $\mu\text{g/mL}$, respectively [38]. The diphenyl ether triclosan has an MIC of 5 $\mu\text{g/mL}$ (17.4 μM) for *M. tuberculosis* [32].

To understand the basis of the mechanism of antitubercular activity of the diphenyl ether derivatives synthesized for this study, molecular modeling and docking studies were

performed. The crystal structure of *E. coli* ENR– NAD^+ –triclosan complex (1C14.pdb) at a resolution of 2.0 Å [39] was optimized and minimized as shown in Fig. 2A with triclosan in ball and stick form and the amino acid residue of NAD^+ below. It showed that triclosan bound non-covalently in the location adjacent to the nicotinamide portion of NAD^+ and formed a parallel stack with nicotinamide ring of the cofactor with an interplanar distance of 3.4 Å. Analysis of the Ramachandran plot shows a normal distribution of points without any amino acid residues classified as outliers. PHI angles were restricted to negative values, and PSI values were clustered in two distinct regions. Several glycine residues had PHI angle values outside the recommended range, but this amino acid is not subjected to the same steric constraints as other residues due to their lack of a side chain. Analysis of the local geometry of the structure, which measures deviations from acceptable bond lengths and bond angles, indicated a robust model with all amino acids within the core region, except 22 residues within the allowable region. No amino acid had bond lengths or angles exceeding the acceptable range.

The binding domain identified to accommodate triclosan is large enough to hold the diphenyl ether derivatives synthesized in this study, although these molecules occupy a larger volume than triclosan (Table 3). In particular, the rings with *ortho* substitutions are larger. The *meta* and *para* substituted structures are also more voluminous than triclosan but could still fit within the binding domain of *E. coli* ENR as observed from the docking results. The potential binding of these structures was determined by a virtual docking procedure using the program FlexX [40,41] in combination with CScore commonly used for virtual high-throughput screening projects [42,43] (Table 2). The diphenyl ether with triazole thione at *meta* position, compound **7b**, had the highest docking score of 65.81% while the substituted pyrazoline ring at *meta* position, compound **9**, of diphenyl ether showed the least docking score of 47.27% indicating that larger molecular volume might result in low docking score.

The diphenyl ethers used in this study occupy a larger molecular volume than triclosan (Table 3), therefore, their cyclic azole substitutions tend to extend beyond the binding domain when positions in order to retain the critical interactions with NAD^+ . Fig. 2A shows the position of triclosan (ball and stick) relative to NAD^+ , Fig. 2B shows the overlay of highest scoring 3-triazole thione diphenyl ether derivative (ball and stick), Fig. 2C, the overlay of least scoring pyrazoline derivative of diphenyl ether (ball and stick) and Fig. 2D the overlap of all 10 derivatives of diphenyl ether **5a**, **5b**, **5c** in wire, **7a**, **7b**, **7c** in stick, **9** in yellow highlighted and **10a**, **10b**, and **10c** in ball and stick form within the binding domain of triclosan diphenyl ether derivative. Changing the spatial orientation of the derivatives to fit more correctly in the pocket precludes or disrupts the π – π stacking interaction that is critical for sustaining the inhibitory activity of diphenyl ethers [27,44]. The stabilization of the ENR–diphenyl ether– NAD^+ complex obtained via the ether oxygen is not possible.

Table 1
Structures of the compounds synthesized and some of their physical properties

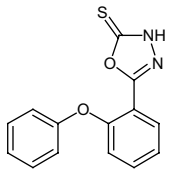
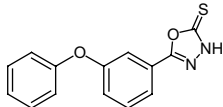
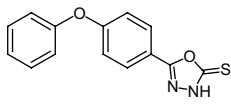
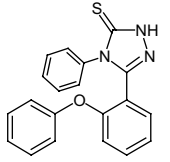
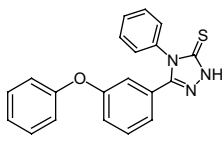
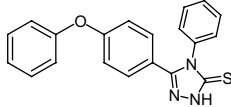
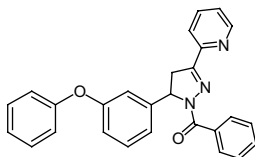
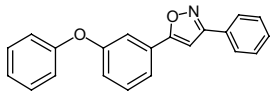
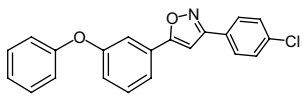
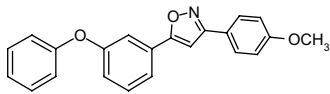
Code	Structure	Mw	Yield (%)	M.p (°C)	Elemental analysis
					Calculated (found)
5a		270.31	87	122	C-62.21% (62.19%) H-3.73% (3.53%) N-10.36% (10.25%)
5b		270.31	85	154	C-62.21% (62.19%) H-3.73% (3.63%) N-10.36% (10.35%)
5c		270.31	70	190	C-62.21% (62.19%) H-3.73% (3.53%) N-10.36% (10.25%)
7a		345.42	88	270	C-69.54% (69.55%) H-4.38% (4.36%) N-12.17% (12.16%)
7b		345.42	86	268	C-69.54% (69.55%) H-4.38% (4.36%) N-12.17% (12.16%)
7c		345.42	78	188	C-69.54% (69.55%) H-4.38% (4.36%) N-12.17% (12.16%)
9		419.47	65	130	C-77.31% (77.11%) H-5.05% (5.00%) N-10.02% (10.00%)
10a		313.35	65	78	C-80.49% (80.39%) H-4.82% (4.83%) N-4.47% (4.45%)
10b		347.79	70	82	C-72.52% (72.49%) H-4.06% (4.03%) N-4.03% (4.05%)
10c		343.38	60	100	C-80.75% (80.69%) H-4.52% (4.53%) N-4.48% (4.45%)

Table 2

Biological activity of the diphenyl ether derivatives against H37Rv strain of *M. tuberculosis* and their docking scores

Code	<i>M. tuberculosis</i> inhibition ^a (%)	Docking score ^b
5a	100	54.16
5b	100	59.18
5c	100	54.39
7a	100	52.77
7b	100	65.81
7c	100	63.79
9	100	47.27
10a	100	58.56
10b	100	54.75
10c	100	52.77
Triclosan	100	98.96

^a At 1 µg/mL concentration, which corresponds to 2.4–3.7 µM.

^b Based on CScore values.

5. Experimental section

5.1. General

Reagents. All reagents were purchased from Sigma Chemicals (Bangalore, India) and were used without further purification.

TLC analysis. Carried out on aluminum foil precoated with silica gel 60 F254 (Sigma–Aldrich Company, Bangalore dealer).

Equipments. Melting points were determined on Toshniwal apparatus (Toshniwal Company, Bangalore, India) and are uncorrected. IR spectra were taken on Shimadzu FTIR 8300 spectrometer. ¹H NMR spectra were recorded on a Bruker AMX-400 NMR spectrometer and were referenced to TMS and all chemical shifts are reported as δ (ppm) values. Compounds were also analyzed by GC–MS (QP 5010, Shimadzu Corporation, Japan), LC–MS, FAB–MS (Joel SX-102, CDRI, Mumbai, India) and EI–MS (Autospec-5, IICT, Hyderabad, India).

5.2. Synthesis of oxadiazolethione

Phenoxy benzaldehyde (*o*/*m*/*p*) **1** (0.01 mol) was oxidized to phenoxy benzoic acid **2** (Scheme 1) using alkaline KMnO₄ solution as per the procedure given in *Vogel's Text Book of Practical Organic Chemistry* [45]. (*o*/*m*/*p*) Phenoxy benzoic acid (0.01 mol) was converted to the respective ester **3** (*o*/*m*/*p*) using methanol, concentrated H₂SO₄, and (*o*/*m*/*p*) phenoxy benzoic acid ester (0.01 mol) to hydrazide **4** (*o*/*m*/*p*) using hydrazine hydrate as per the procedure given in Ref. [46].

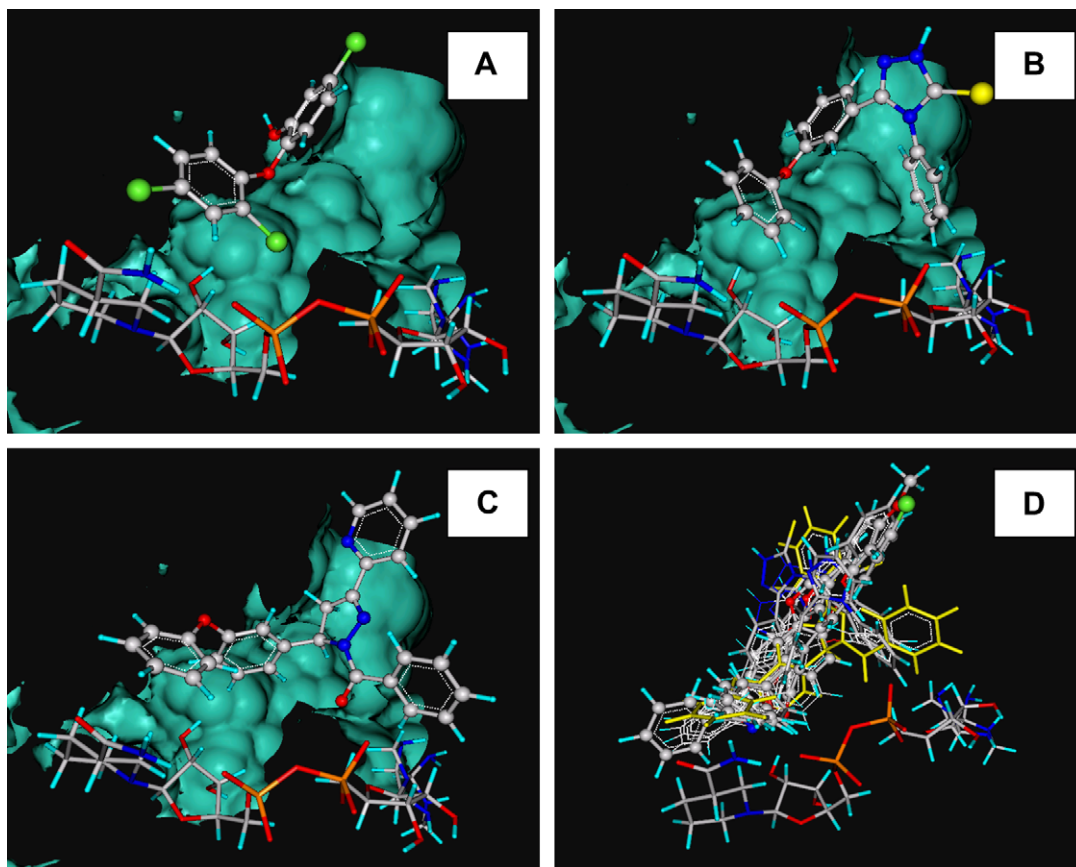


Fig. 2. Binding domain of *E. coli* ENR showing (A) the position of triclosan (ball and stick) relative to NAD⁺, (B) the overlay of highest scoring 3-triazole thione diphenyl ether derivative (ball and stick), (C) the overlay of least scoring pyrazoline derivative of diphenyl ether (ball and stick) and (D) the overlap of all 10 derivatives of diphenyl ether **5a**, **5b**, **5c** in wire, **7a**, **7b**, **7c** in stick, **9** in yellow highlights and **10a**, **10b**, and **10c** in ball and stick form within the binding domain of triclosan (for interpretation of the references to colour in this figure legend, the reader is referred to the web version of this article).

Table 3
Molecular properties of the diphenyl ethers used in this study

Code	Mw	Volume, Å ³	Dipole, Debye	E_{total} , kcal/mol	IP, eV	e_{HOMO} , eV	e_{LUMO} , eV	EP _{min} , eV	EP _{max} , eV	LP _{min}	LP _{max}
5a	270.31	258.95	7.18	12.088	8.589	−8.793	−0.384	−26.253	28.637	0.106	0.178
5b	270.31	262.38	6.16	12.353	8.706	−8.925	−0.387	−25.278	32.249	0.109	0.182
5c	270.31	262.37	3.08	12.369	8.697	−8.902	−0.369	−25.746	30.978	0.111	0.181
7a	345.42	321.97	4.17	26.430	8.150	−8.240	−0.308	−27.539	24.782	0.114	0.170
7b	345.42	326.84	3.43	26.866	8.254	−8.357	−0.354	−26.529	28.016	0.116	0.172
7c	345.42	326.61	3.16	26.871	8.251	−8.352	−0.355	−26.906	26.570	0.117	0.172
9	419.47	409.08	3.00	12.785	9.053	−9.429	−0.059	−40.750	29.375	0.067	0.126
10a	313.35	317.63	2.35	13.453	9.253	−9.462	−0.136	−29.532	16.845	0.113	0.154
10b	347.79	334.91	2.93	13.029	9.309	−9.702	−0.399	−28.267	18.111	0.123	0.198
10c	343.38	352.81	3.22	15.156	9.276	−9.597	−0.275	−32.607	20.167	0.094	0.148
Triclosan	289.54	246.43	1.99	2.662	9.700	−9.251	−0.201	−22.831	32.121	0.167	0.263

Note: volume = connolly solvent accessible surface volume; E_{total} = total energy; IP = ionization energy; e_{HOMO} = energy of highest occupied molecular orbital; e_{LUMO} = energy of lowest unoccupied molecular orbital; EP_{max} and EP_{min} = maximum and minimum electrostatic potentials; LP_{max} and LP_{min} = maximum and minimum lipophilicities.

A mixture of equimolar quantities (0.01 mol) of (*o*/*m*/*p*) phenoxy benzoic acid hydrazide, CS₂ and KOH were taken in absolute ethanol in a round bottom flask. The solution was refluxed until the evolution of H₂S had nearly stopped (about 18 h). The solvent was removed under reduced pressure. The residue was dissolved in water and the solution was acidified with dilute HCl (10%). The resulting product **5** was collected, washed with water, dried and recrystallized from aqueous ethanol (80%). The purity of the compound was ascertained by a single spot on the TLC plate. The physical and molecular data are given in Tables 1 and 3. The solvent system for TLC was chloroform:methanol (8:2 v/v).

5.3. Synthesis of triazole thione

Equimolar quantities (0.01 mol) of acid hydrazide and phenyl isothiocyanate were dissolved in absolute ethanol in a round bottom flask (Scheme 1). The solution was refluxed for 3 h on a water bath. The solution was concentrated under reduced pressure and the solid separated was collected and recrystallized from appropriate solvent to get the isothiocyanate derivative **6**. This was further used to prepare triazole whereby it was suspended in 4% NaOH and refluxed for 1 h (Scheme 1). The resulting solution was filtered and the filtrate was cooled, acidified carefully with diluted acetic acid to pH 5.5. The precipitate formed was filtered, washed with water, and the product **7** was crystallized from ethanol. The purity of the compounds was established by single spot on the TLC plate. The physical and molecular data are given in Tables 1 and 3. The solvent system used consisted of chloroform:ethyl acetate (1:1 v/v).

5.4. Synthesis of isoxazole derivatives

Preparation of chalcone. *m*-Phenoxy benzaldehyde **1** (0.01 mol) in ethanol (95%, 15.0 mL) was added to the mixture of acetophenone (0.01 mol), ethanol (95%, 20.0 mL) and NaOH (40%, 8.0 mL) and stirred for 24 h (Scheme 2). The content was poured into crushed ice. The product was isolated by acidification and crystallization from ethanol (95%).

Anhydrous sodium acetate (0.01 mol) dissolved in a minimum amount of hot acetic acid was added to the solution of hydroxylamine hydrochloride (0.01 mol) in ethanol (15.0 mL). This solution was added to a solution of chalcone (0.01 mol) in ethanol (20.0 mL). The mixture was refluxed on an oil-bath for 8 h, concentrated and neutralized with NaOH solution (0.1%). The product **10** was crystallized from ethanol (95%). The physical and molecular data are given in Tables 1 and 3.

5.5. Synthesis of pyrazoline derivatives

m/*p* Phenoxy benzaldehyde (0.01 mol) was dissolved in 15 mL of ethanol. 2-Methylpyridyl ketone dissolved in 15 mL of ethanol was added (Scheme 1). This mixture was kept on a magnetic stirrer and slowly a stream of NaOH solution (40%, 10 mL) was added and stirred overnight. The mixture was then acidified to pH 5.0 to obtain the chalcone. The precipitate was filtered, dried and crystallized from ethanol. This chalcone **8** was used to prepare different pyrazolines. The hydrazide of the benzoic acid was synthesized by the usual method.

The above-prepared chalcone (0.01 mol) was dissolved in ethanol (15 mL). The hydrazide of the benzoic acid (0.01 mol) was dissolved in ethanol (20 mL) and added. To this mixture few drops of glacial acetic acid was added and the mixture was refluxed for 12 h. The solvent was then removed under reduced pressure and the product was poured into ice-cold water. The precipitate of pyrazoline (**9**) was obtained which was filtered and dried. The product was crystallized from ethanol. The physical and molecular data are given in Tables 1 and 3. The solvent system for TLC was benzene:ethylacetate (1:2 v/v).

5.6. Spectral data

5.6.1. 5-(3-Phenoxyphenyl)-1,3,4-oxadiazole-2(3H)-thione

FTIR spectral data. KBr pellet: C=N (1583.4), C=S (1180.4), C—O stretch (1693.4), C—O—C (oxadiazole)

(1336.6), C–O–C (diphenyl ether) (1232.4), Ar stretch (688.5), N–H (3456.2).

^1H NMR (DMSO). δ 8.3 (s, 1H, NH of oxadiazole), δ 6.9–7.9 (m, 9H, Ar).

Mass calculated for $\text{C}_{14}\text{H}_{10}\text{N}_2\text{O}_2\text{S}$ 270.0, found 270.0.

5.6.2. 5-(2-Phenoxyphenyl)-4-phenyl-2,4-dihydro-3H-1,2,4-triazole-3-thione

FTIR spectral data. KBr pellet: C=N (1577.7), C=S (1157.2), C–N stretch (1612.4), C–N–C (1394.4), C–O–C (diphenyl ether) (1242.1), Ar stretch (692.4), N–H (3436.9).

^1H NMR (DMSO). δ 3.2 (s, 1H, triazole), δ 6.7–7.7 (m, 14H, Ar).

Mass calculated for $\text{C}_{20}\text{H}_{15}\text{N}_3\text{OS}$ 345.1 and molecular ion ($m + 1$) peak from LC–MS was obtained at 346.14.

5.6.3. 3-(4-Methoxyphenyl)-5-(3-phenoxyphenyl)isoxazole

FTIR spectral data. KBr pellet: C=N (1579.6), C=C (isoxazole) (1515.9), C–O stretch (1614.3.6), CH_3 (1461.9), C–O–C (diphenyl ether) (1245.9), Ar stretch (692.4).

^1H NMR (DMSO). δ 2.3 (s, 1H, CH), δ 6.9–8.0 (m, 13H, Ar), δ 3.8 (s, 1H, CH_3).

Mass calculated for $\text{C}_{22}\text{H}_{17}\text{NO}_3$ is 343.37 and molecular ion peak was obtained at 343 indicating that the compound is formed.

5.6.4. 2-[5-(3-Phenoxyphenyl)-4,5-dihydro-1(benzoyl)-pyrazol-3-yl] pyridine

FTIR spectral data. KBr pellet: C=N (1442.7), C=O (1685.7), C–O–C (diphenyl ether) (1242.1), Ar stretch (694.3, 3055).

^1H NMR (DMSO). δ 6.9–8.5 (m, 17H), δ 3.2 and 4.0 (d, CH_2), δ 4.2 and 5.0 (d, CH).

Mass calculated for $\text{C}_{27}\text{H}_{22}\text{N}_3\text{O}_3$ is 435.23 and molecular ion ($m + 1$) peak was obtained at m/z 436.23. The other fragment peaks were obtained at m/z 316.2, 269.2, 121.1.

Acknowledgements

We are thankful to the Microbiology Department of Kasturba Medical College, Manipal for helping with the anti-tubercular assay, and to the Central Drug Research Institute, Lucknow; Indian Institute of Science, Bangalore and Indian Institute of Chemical Technology, Hyderabad for providing the elemental analysis, ^1H NMR and mass spectra of the compounds. Portions of molecular modeling work were funded at Department of Medicinal Chemistry, University of Mississippi, University, MS 38677, USA by Centers for Diseases Control Cooperative Agreements U50/CCU18839 and UR3/CCU418652, and supported by National Institutes of Health (NIH) MFGN INBRE RR016476 and NIH NCRR Facilities Improvement grant CO6 RR1450301.

References

- [1] E. Wolinsky, in: J.B. Wyngaarden, L.H. Smith Jr., J.C. Bennett (Eds.), Tuberculosis, 19th ed., Cecil Textbook of Medicine, vol. 2 W.B. Saunders Company, Philadelphia, PA, 1992, pp. 1733–1742.
- [2] P. Sensi, I.G.G. Grass, in: A. Burger, M.E. Wolff (Eds.), Antimycobacterial Agents, fifth ed., Burger's Medicinal Chemistry and Drug Discovery, vol. 2 John Wiley & Sons, New York, 1996, pp. 575–635.
- [3] B.R. Bloom, C.J.L. Murray, Tuberculosis: commentary on a reemerging killer, Science 257 (1992) 1055–1064.
- [4] M. Okada, K. Kobayashi, Recent progress in mycobacteriology, Kekkaku (Japanese Journal) 82 (10) (2007) 783–799.
- [5] World Health Organization Report on TB epidemic, Global TB Programme, World Health Organization, Geneva, 1997.
- [6] World Health Organisation, Tuberculosis, Fact Sheet No. 104, 2007 (site accessed: <www.who.int/mediacentre/factsheets/fs104/en/index.html>).
- [7] K.A. ElSayed, P. Bartyzel, X.Y. Shen, T.L. Perry, J.K. Zjawiony, M.T. Hamann, Marine natural products as antituberculosis agents, Tetrahedron 56 (2000) 949–953.
- [8] M.J. Goldberg, Antituberculosis agents, Med. Clin. North. Am. 72 (1988) 661–668.
- [9] H. Tomioka, K. Namba, Development of antitubercular drugs: current status and future prospects, Kekkaku (Japanese Journal) 81 (12) (2006) 753–774.
- [10] S.E. Berning, The role of fluoroquinolones in tuberculosis today, Drugs 61 (2001) 9–18.
- [11] V.M. Reddy, G. Nadadur, D.D. Daneluzzi, J.F. Osullivan, P.R.J. Gangadharam, Antituberculosis activities of clofazimine and its new analogs B4154 and B4157, Antimicrob. Agents Chemother. 40 (1996) 633–636.
- [12] C.E. Barry, New horizons in the treatment of tuberculosis, Biochem. Pharmacol. 54 (1997) 1165–1172.
- [13] K.F.M. Pasquato, E.I. Ferreira, An approach for the rational design of new antitubercular agents, Curr. Drug Targets 2 (2001) 427–437.
- [14] E.K. Schroeder, N. de Souza, D.D. Santos, J.S. Blanchard, L.A. Basso, Drugs that inhibit mycolic acid biosynthesis in *Mycobacterium tuberculosis*, Curr. Pharm. Biotechnol. 3 (3) (2002) 197–225.
- [15] C.E. Barry III, R.E. Lee, K. Mdluli, A.E. Sampson, B.G. Schroeder, R.A. Slayden, Y. Yaun, Mycolic acid structure, biosynthesis and physiological functions, Prog. Lipid Res. 37 (1998) 143–179.
- [16] P.E. Kolattukudy, N.D. Fernandes, A.K. Azad, A.M. Fitzmaurice, T.D. Sirakova, Biochemistry and molecular genetics of cell-wall lipid biosynthesis in mycobacteria, Mol. Microbiol. 24 (1997) 263–270.
- [17] H. Bergler, S. Fuchsbichler, G. Hogenauer, F. Turnowsky, The enoyl-[acyl-carrier-protein] reductase (FabI) of *Escherichia coli*, which catalyzes a key regulatory step in fatty acid biosynthesis, accepts NADH and NADPH as cofactors and is inhibited by palmitoyl-CoA, Eur. J. Biochem. 242 (1996) 689–694.
- [18] M.J. Stewart, S. Parikh, G. Xiao, P.J. Tonge, C. Kisker, Structural basis and mechanism of enoyl reductase inhibition by triclosan, J. Mol. Biol. 290 (1999) 859–865.
- [19] D.A. Rozwarski, C. Vilcheze, M. Sugantino, R. Bittman, J.C. Sacchettini, Crystal structure of the *Mycobacterium tuberculosis* enoyl-ACP reductase, InhA, in complex with NAD^+ and a C16 fatty substrate, J. Biol. Chem. 274 (1999) 15582–15589.
- [20] H.I. Boshoff, V. Mizrahi, C.E. Barry III, Effects of pyrazinamide on fatty acid synthesis by whole mycobacterial cells and purified fatty acid synthase I, J. Bacteriol. 184 (2002) 2167–2172.
- [21] O. Zimhony, J.S. Cox, J.T. Welch, C. Vilcheze, W.R. Jacobs Jr., Pyrazinamide inhibits the eukaryotic-like fatty acid synthetase I (FAS I) of *Mycobacterium tuberculosis*, Nat. Med. 6 (2000) 1043–1047.
- [22] H.P. Schweizer, Triclosan: a widely used biocide and its link to antibiotics, FEMS Microbiol. Lett. 202 (2001) 1–7.
- [23] J. Regos, O. Zak, R. Solf, W.A. Vischer, E.G. Weirich, Antimicrobial spectrum of triclosan, a broad-spectrum antimicrobial agent for topical application. II. Comparison with some other antimicrobial agents, Dermatologica 1158 (1979) 72–79.

- [24] W.A. Vischer, J. Regos, Antimicrobial spectrum of triclosan, a broad-spectrum antimicrobial agent for topical application, *Zentralbl. Bakteriol. [Orig. A]* 226 (1974) 376–389.
- [25] L.M. McMurtry, M. Oethinger, S.B. Levy, Triclosan targets lipid synthesis, *Nature* 394 (1998) 531–532.
- [26] R.J. Heath, Y.T. Yu, M.A. Shapiro, E. Olson, C.O. Rock, Broad spectrum antimicrobial biocides target the FabI component of fatty acid synthesis, *J. Biol. Chem.* 273 (1998) 30316–30320.
- [27] C.W. Levy, A. Roujeinikova, S. Sedelnikova, P.J. Baker, A.R. Stuitje, Molecular basis of triclosan activity, *Nature* 398 (1999) 383–384.
- [28] A. Roujeinikova, C.W. Levy, S. Rowsell, S. Sedelnikova, P.J. Baker, C.A. Minshull, A. Mistry, J.G. Colls, R. Camble, A.R. Stuitje, A.R. Slabas, J.B. Rafferty, R.A. Paupit, R. Viner, D.W. Rice, Crystallographic analysis of triclosan bound to enoyl reductase, *J. Mol. Biol.* 294 (1999) 527–535.
- [29] R.J. Heath, J. Li, G.E. Roland, C.O. Rock, Inhibition of the *Staphylococcus aureus* NADPH-dependent enoyl-acyl carrier protein reductase by triclosan and hexachlorophene, *J. Biol. Chem.* 275 (2001) 4654–4659.
- [30] J. Marcinkeviciene, W. Jiang, L.M. Kopcho, G. Locke, Y. Luo, Enoyl-ACP reductase (FabI) of *Haemophilus influenzae*: steady-state kinetic mechanism and inhibition by triclosan and hexachlorophene, *Arch. Biochem. Biophys.* 390 (2001) 101–108.
- [31] L.M. McMurtry, P.F. McDermott, S.B. Levy, Genetic evidence that InhA of *Mycobacterium smegmatis* is a target for triclosan, *Antimicrob. Agents Chemother.* 43 (1999) 711–713.
- [32] S.L. Parikh, G. Xiao, P.J. Tonge, Inhibition of InhA, the enoyl reductase from *Mycobacterium tuberculosis*, by triclosan and isoniazid, *Biochemistry* 39 (2000) 7645–7650.
- [33] M.R. Kuo, H.R. Morbidoni, D. Alland, S.F. Sneddon, B.B. Gourlie, Targeting tuberculosis and malaria through inhibition of enoyl reductase: compound activity and structural data, *J. Biol. Chem.* 278 (2003) 20851–20859.
- [34] N. Surolia, A. Surolia, Triclosan offers protection against blood stages of malaria by inhibiting enoyl-ACP reductase of *Plasmodium falciparum*, *Nat. Med.* 7 (2001) 167–173.
- [35] M. Kapoor, M.J. Dar, N. Surolia, A. Surolia, Kinetic determinants of the interaction of enoyl-ACP reductase from *Plasmodium falciparum* with its substrates and inhibitors, *Biochem. Biophys. Res. Commun.* 289 (2001) 832–837.
- [36] R. Perozzo, M. Kuo, A. bir Singh Sidhu, J.T. Valiyaveetil, R. Bittman, W.R. Jacobs Jr., D.A. Fidock, J.C. Sacchettini, Structural elucidation of the specificity of the antibacterial agent triclosan for malarial enoyl ACP reductase, *J. Biol. Chem.* 277 (2002) 13106.
- [37] C.B. Vincent, D. Twomey, Derivatives of diploicin, *Proc. Royal Irish Acad.* 53B (1950) 55–59.
- [38] Dosages and Pharmacokinetics of Antituberculosis medications – A Report in India, 13.06.2006 (site accessed: <<http://www.angelfire.com/indie/tbindia/attdrugs.html>>).
- [39] X. Qiu, C.A. Janson, R.I. Court, M.G. Smyth, D.J. Payne, S.S. Abdel-Meguid, Molecular basis for triclosan activity involves a flipping loop in the active site, *Protein Sci.* 8 (1999) 2529–2532.
- [40] M. Rarey, B. Kramer, T. Lengauer, G.A. Klebe, Fast flexible docking method using an incremental construction algorithm, *J. Mol. Biol.* 261 (1996) 470–489.
- [41] B. Kramer, M. Rarey, T. Lengauer, Evaluation of the FlexX incremental construction algorithm for protein–ligand docking. Proteins: structure, function, and genetics, *J. Mol. Biol.* 37 (1999) 228–241.
- [42] C. Bissantz, G. Folkers, D. Rognan, Protein-based virtual screening of chemical databases. Part 1. Evaluation of different docking/scoring combinations, *J. Med. Chem.* 43 (2000) 4759–4767.
- [43] R.J. Heath, J.R. Rubin, D.R. Holland, E. Zhang, M.E. Snow, C.O. Rock, Mechanism of triclosan inhibition of bacterial fatty acid synthesis, *J. Biol. Chem.* 274 (1999) 11110–11114.
- [44] S. Sivarana, T.J. Sullivan, F. Johnson, P. Novichenok, G. Cui, C. Simmerling, P.J. Tonge, Inhibition of the bacterial enoyl reductase FabI by triclosan: a structure–reactivity analysis of FabI inhibition by triclosan analogues, *J. Med. Chem.* 47 (2004) 509–518.
- [45] B.S. Furniss, A.J. Hannaford, V. Rogers, P.W.G. Smith, A.R. Tatchell, Aromatic carboxylic acids, Vogel's Text Book of Practical Organic Chemistry, fourth ed. Longman Group Limited, London, 1980, p. 824.
- [46] R. Udipi, Studies on the Synthesis of Substituted Triazoles, Azetidiones, Quinazolinones and Related Compounds for Possible Antitubercular Activity and other Pharmacological Profiles, Ph.D. Thesis, 1995.
- [47] B. Watt, A. Rayner, G. Harris, Mackie, McCartney, in: J.G. Colle, A.G. Fraser, B.P. Marmion, A. Simmons (Eds.), *Practical Medical Microbiology*, Churchill Livingstone, New York, 1996, pp. 331–335 (Chapter18).
- [48] J.T. Edsall, P.J. Flory, J.C. Kendrew, A.M. Liquori, G. Nemethy, G.N. Ramachandran, H.A. Scheraga, A proposal of standard conventions and nomenclature for the description of polypeptide conformations, *J. Biol. Chem.* 241 (1966) 1004–1008.
- [49] W. Purcell, J.A. Singer, Brief review and table of semiempirical parameters used in the Hueckel molecular orbital method, *J. Chem. Eng. Data.* 12 (1967) 235–246.
- [50] P. Cieplak, W.D. Cornell, C. Bayly, P.A. Kollman, Application of the multimolecule and multiconformational RESP methodology to biopolymers: charge derivation for DNA, RNA, and proteins, *J. Comput. Chem.* 16 (1995) 1357–1377.
- [51] A.R. Leach, I. Kuntz, Conformational analysis of flexible ligands in macromolecular receptor sites, *J. Comput. Chem.* 13 (1992) 730–748.
- [52] M. Rarey, B. Kramer, T. Lengauer, Multiple automatic base selection: protein–ligand docking based on incremental construction without manual intervention, *J. Comput.-Aided Mol. Des.* 11 (1997) 369–384.